Joint Channel and Symbol Estimation by Oblique Projections

Xiang Yu and Lang Tong*
School of Electrical Engineering
Cornell University, Ithaca, NY 14853
e-mail:{xiang,ltong}@ee.cornell.edu

Abstract — **The problem of simultaneous channel and symbol estimation of a single input multiple output communication channel is considered in this paper. Three new deterministic algorithms are developed based on oblique projections of the observation onto past and future output subspaces. Also proposed is a channel order detection algorithm which improves the estimation performance significantly for multipath channels.**

I. Introduction

Joint channel and symbol estimation has important applications in packet transmissions where the use of training symbols may impose substantial overhead. Most existing techniques are iterative algorithms based on the maximization of likelihood function [5]. Unfortunately, these techniques require good initializations. Recently, Vandaele and Moonen [8] proposed a new algorithm that provides simultaneous channel and symbol estimation in closed-form. The key of their approach is the use of a specific oblique projection which, in contrast to other techniques based on orthogonal projections (see [6, 10] and references therein), provides the finite sample convergence property [6] to both channel and symbol estimation.

In this paper, based on elementary geometrical characterizations of input-output subspaces, we present a systematic use of oblique projections for joint channel and symbol estimation, which leads to three new estimators and a channel order detection technique.

II. Preliminaries

Problem Statement Consider the following single input P output system:

$$\mathbf{x}(t)=\sum_{l=0}^{L}\mathbf{h}_l s(t-l),\ \mathbf{y}(t)=\mathbf{x}(t)+\mathbf{n}(t), t=1,\cdots,N, \quad (1)$$

where $s(t)$ is the input complex sequence, $\mathbf{x}(t)$ the noiseless output, and $\mathbf{h}_l$ the vector channel impulse response. With additive noise $\mathbf{n}(t)$, the received signal is $\mathbf{y}(t)$. Our goal is to estimate both the channel $\mathbf{h}\triangleq[\mathbf{h}_L^T,\cdots,\mathbf{h}_0^T]^T$ and the symbols $s(t)$ from $\mathbf{y}(t)$.

We will use the block representation of the above SIMO model by stacking m samples of $\mathbf{x}(t)$ and denoting $\mathbf{x}_m(t)\triangleq[\mathbf{x}^T(t),\cdots,\mathbf{x}^T(t-m+1)]^T$. We then have

$$\mathbf{x}_m(t)=\mathcal{F}_m(\mathbf{h})\mathbf{s}_{L+m}(t),\quad \mathbf{y}_m(t)=\mathbf{x}_m(t)+\mathbf{n}_m(t), \quad (2)$$

where $\mathcal{F}_m(\mathbf{h})$ is the filtering matrix

$$\mathcal{F}_m(\mathbf{h})\triangleq\begin{pmatrix}\mathbf{h}_0 & \cdots & \mathbf{h}_L & & \\ & \ddots & \cdots & \ddots & \\ & & \mathbf{h}_0 & \cdots & \mathbf{h}_L\end{pmatrix}_{mP\times(m+L)} \quad (3)$$

and $\mathbf{y}_m(t),\mathbf{n}_m(t)$ and $\mathbf{s}_{L+m}(t)$ are similarly defined as $\mathbf{x}_m(t)$.

We make the following two assumptions:

- A1 There exists a m_0 such that the filtering matrix $\mathcal{F}_{m_0}$ has full column rank.
- A2 The input sequence $s(t)$ has linear complexity [2] greater than $L_*=2m_0+2L$.

Assumptions A1 and A2 play a critical role in all subspace methods; they imply an isomorphic relation between the (noiseless) output and input subspaces. Note also that this relation is valid for all $m\geq m_0$.

Most notations in this paper are standard. The upper and lower-case bold letters denote matrices and vectors, respectively. $(\cdot)^T$ and $(\cdot)^H$ are the transpose and Hermitian operators. $(\cdot)^\dagger$ denotes the Moore-Penrose pseudo-inverse of the matrix. For a given matrix $\mathbf{A}$, $\mathcal{R}\{\mathbf{A}\}$ ($\mathcal{C}\{\mathbf{A}\}$) is the row (column) space of the matrix. Calligraphic letters denote subspaces. For a given subspace $\mathcal{R}$, $\mathbf{P}_{\mathcal{R}}$ ($\mathbf{P}_{\mathcal{R}}^{\perp}$) denotes the corresponding orthogonal (complement) projection matrix and $\mathbf{x}_{|\mathcal{R}}$ denotes the orthogonal projection of $\mathbf{x}$ onto $\mathcal{R}$. For two given subspaces $\mathcal{R}$ and $\mathcal{N}$, $\mathbf{E}_{\mathcal{R},\mathcal{N}}$ denotes the corresponding oblique projection matrix with $\mathcal{R}$ as the range space and $\mathcal{N}$ as the null space. For a set of vectors $\mathbf{x}_1,\cdots,\mathbf{x}_n$, $sp\{\mathbf{x}_1,\cdots,\mathbf{x}_n\}$ denotes the linear subspace spanned by $\mathbf{x}_1,\cdots,\mathbf{x}_n$. $\|\cdot\|$ is the 2-norm.

Oblique Projection The oblique projection [1, 4] obtains the component of a vector in a particular direction. Specifically, consider subspaces $\mathcal{Z}_{\mathcal{R}}$, $\mathcal{Z}_{\mathcal{N}}$ and $\mathcal{Z}=\mathcal{Z}_R\oplus\mathcal{Z}_N$ in $\mathcal{C}^n$ and an arbitrary vector $\mathbf{x}\in\mathcal{C}^n$ as illustrated in Fig. 1. The oblique projection of $\mathbf{x}$ onto $\mathcal{Z}_R$ along $\mathcal{Z}_N$, denoted by $\mathbf{x}_{\mathcal{Z}_R|\mathcal{Z}_N}$, is obtained by (i) the orthogonal projection $\mathbf{x}_{|\mathcal{Z}}$ of $\mathbf{x}$ onto $\mathcal{Z}$, (ii) finding the component of $\mathbf{x}_{|\mathcal{Z}}$ in the direction of $\mathcal{Z}_R$. In particular, if $\mathcal{Z}_R$ is the column space of matrix $\mathbf{R}$ and $\mathcal{Z}_N$ the column space of matrix $\mathbf{N}$, then

$$\mathbf{x}_{\mathcal{Z}_R|\mathcal{Z}_N}=\mathbf{E}_{\mathcal{Z}_R,\mathcal{Z}_N}\mathbf{x}$$

where $\mathbf{E}_{\mathcal{Z}_R,\mathcal{Z}_N}$ is the projection operator given by

$$\mathbf{E}_{\mathcal{Z}_R,\mathcal{Z}_N}=(\mathbf{R}\quad\mathbf{0})(\mathbf{R}\quad\mathbf{N})^\dagger. \quad (4)$$

Being a projection, any vector in its range space will be preserved, *i.e.*, for $\mathbf{x}\in\mathcal{Z}_R$, $\mathbf{E}_{\mathcal{Z}_R,\mathcal{Z}_N}\mathbf{x}=\mathbf{x}$. Furthermore, for $\mathbf{x}\in\mathcal{Z}_N\oplus\mathcal{Z}^\perp$, $\mathbf{E}_{\mathcal{Z}_R,\mathcal{Z}_N}\mathbf{x}=\mathbf{0}$, i.e. the projector on $\mathcal{Z}_R$ along $\mathcal{Z}_N$ preserves any vector in $\mathcal{Z}_R$ and nulls any vector in $\mathcal{Z}_N\oplus\mathcal{Z}^\perp$. Note also that obtaining the oblique projection of vector $\mathbf{x}$ is equivalent to solving a least squares problem, which can be implemented by standard recursive techniques.

*This work was supported in part by the National Science Foundation under Contract CCR-9804019 and by the Office of Naval Research under Contract N00014-96-1-0895

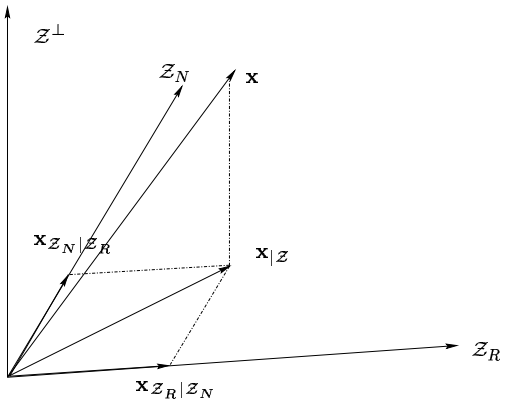

Figure 1: Oblique Projection Illustration: The oblique projection of $\mathbf{x}$ onto $\mathcal{Z}_\mathcal{R}$ along $\mathcal{Z}_\mathcal{N}$ is $\mathbf{x}_{\mathcal{Z}_\mathcal{R}|\mathcal{Z}_\mathcal{N}}$

.

III. ISI Removal by Oblique Projections

The joint channel and symbol estimation relies on the isomorphic relation between the input and output subspaces. Specifically, define

$$\mathbf{s}_t \triangleq [s(t), s(t+1), \cdots], \quad \mathcal{S}_{t,p} \triangleq sp(\mathbf{s}_t, \cdots, \mathbf{s}_{t-p+1}), \quad (5)$$

$$\mathbf{x}_t \triangleq [\mathbf{x}(t), \mathbf{x}(t+1), \cdots], \quad \mathcal{X}_{t,p} \triangleq sp(\mathbf{x}_t, \cdots, \mathbf{x}_{t-p+1}). \quad (6)$$

Under A1-A2, we have, for $m \geq m_0$,

$$\mathcal{X}_{t,m} = \mathcal{S}_{t,m+L}. \quad (7)$$

This property tells us that any input subspace spanned by no less than $m_0 + L$ consecutive row vectors can be directly constructed from the corresponding output subspace. By this property, we can use such subspace techniques as projection, intersection and union to obtain the estimates of the channel and input symbols.

The Use of Oblique Projection The key idea here is one of smoothing: estimate the component related to the current input from past and future observations. As in the least squares smoothing (LSS) approach [6, 10], we aim to eliminate the interference from past and future input. Specifically, consider $L+1$ consecutive noiseless observations $\mathbf{X}_{L+1}(t+L) \triangleq [\mathbf{x}_{t+L}^T, \cdots, \mathbf{x}_t^T]^T$. From (2), we have

$$\mathbf{X}_{L+1}(t+L) = \begin{pmatrix} \mathbf{h}_0 & \cdots & \mathbf{h}_L & & \\ & \ddots & \cdots & \ddots & \\ & & \mathbf{h}_0 & \cdots & \mathbf{h}_L \end{pmatrix} \begin{pmatrix} \mathbf{s}_{t+L} \\ \vdots \\ \mathbf{s}_{t-L} \end{pmatrix} \quad (8)$$

$$= \mathbf{h}\mathbf{s}_t + \mathbf{J}(t), \quad (9)$$

where the interference

$$\mathbf{J}(t) \triangleq \underbrace{\mathbf{H}_{\mathcal{F}_1}\mathbf{S}_{\mathcal{F}_1}}_{\substack{\text{future} \\ \text{interference}}} + \underbrace{\mathbf{H}_{\mathcal{P}_1}\mathbf{S}_{\mathcal{P}_1}}_{\substack{\text{past} \\ \text{interference}}}. \quad (10)$$

To obtain $\mathbf{h}\mathbf{s}_t$, $\mathbf{X}_{L+1}(t+L)$ needs to be projected onto a signal space containing $\mathbf{h}\mathbf{s}_t$ (but no interference) along the interference space $\mathcal{I}$ that includes the past and future interferences. Once $\mathbf{h}\mathbf{s}_t$ is obtained, its rank-1 decomposition leads to the channel and symbol estimates. Note that, in LSS [10], $\mathbf{X}_{L+1}(t+L)$ is projected onto the orthogonal complement of $\mathcal{I}$ which, in general, does not include $\mathbf{h}\mathbf{s}_t$, hence the lost of finite sample convergence property in the estimator of $\mathbf{s}_t$.

The Past and the Future Subspaces The past and future interferences reside in the subspaces spanned by

$$\mathcal{P}_1 \triangleq \mathcal{S}_{t-1,L+m} = \mathcal{X}_{t-1,m} = \mathcal{R}\{\mathbf{X}_m(t-1)\},$$

$$\mathcal{F}_1 \triangleq \mathcal{S}_{t+L+m,L+m} = \mathcal{X}_{t+L+m,m} = \mathcal{R}\{\mathbf{X}_m(t+L+m)\}.$$

The interference subspace is therefore spanned by $\mathcal{P}_1 \oplus \mathcal{F}_1$. To obtain the subspace that contains $\mathbf{h}\mathbf{s}_t$, we extend the past and future to include current input

$$\mathcal{P}_2 \triangleq \mathcal{P}_1 \oplus sp\{\mathbf{h}\mathbf{s}_t\} = \mathcal{R}\{\mathbf{X}_{m+1}(t)\},$$

$$\mathcal{F}_2 \triangleq \mathcal{F}_1 \oplus sp\{\mathbf{h}\mathbf{s}_t\} = \mathcal{R}\{\mathbf{X}_{m+1}(t+L+m)\}.$$

The row space of the current data $\mathcal{C} = \mathcal{R}\{\mathbf{X}_{L+1}(t+L)\}$ satisfies

$$\mathcal{C} \subset \mathcal{F}_1 \oplus \mathcal{P}_1 \oplus \mathbf{s}_t \quad (11)$$

It is important to note that all these subspaces, as illustrated in Figure 2, can be directly obtained from the observation.

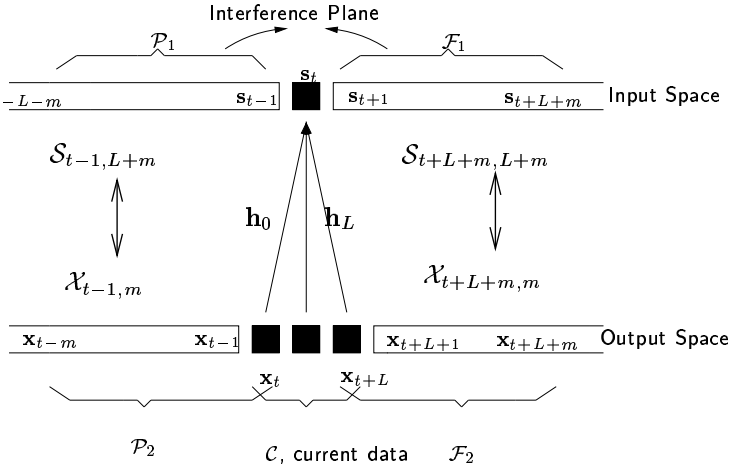

Figure 2: *future, past* and *current* data of the SIMO system.

The Algorithm: The Algebra From the above subspace definitions, we have

$$\mathcal{R}\{\mathbf{h}\mathbf{s}_t\} = \mathcal{P}_2 \bigcap \mathcal{F}_2, \quad \mathcal{R}\{\mathbf{J}(t)\} \subset \mathcal{P}_1 \oplus \mathcal{F}_1,$$

$$\mathbf{X}_{L+1}(t+L) = \mathbf{h}\mathbf{s}_t + \mathbf{J}(t).$$

Therefore, $\mathbf{h}\mathbf{s}_t$ can be obtained from the oblique projection of $\mathbf{X}_{L+1}(t+L)$ onto $\mathcal{P}_2 \bigcap \mathcal{F}_2$ along $\mathcal{P}_1 \oplus \mathcal{F}_1$. To compute this projection, we call the following lemma [4]

Lemma 1 *Let $\mathbf{E}_i$ be a projector onto subspace $\mathcal{R}_i$ along $\mathcal{N}_i$,$i = 1, 2$. Then $\mathbf{E} = \mathbf{E}_1\mathbf{E}_2$ is a projector onto $\mathcal{R} = \mathcal{R}_1 \cap \mathcal{R}_2$ along $\mathcal{N} = \mathcal{N}_1 \oplus \mathcal{N}_2$ if and only if $\mathbf{E}_1\mathbf{E}_2 = \mathbf{E}_2\mathbf{E}_1$.*

Since subspaces $\mathcal{P}_i, \mathcal{F}_i$ can all be obtained from the observation, the above lemma leads directly to an estimation algorithm of $\mathbf{h}\mathbf{s}_t$ by letting $\mathbf{E}_1 = \mathbf{E}_{\mathcal{F}_2,\mathcal{P}_1}$, $\mathbf{E}_2 = \mathbf{E}_{\mathcal{P}_2,\mathcal{F}_1}$. It can be verified that $\mathbf{E}_1$ and $\mathbf{E}_2$ commute. Therefore,

$$\mathbf{h}\mathbf{s}_t = \mathbf{X}_{L+1}(t+L)(\mathbf{E}_{\mathcal{F}_2,\mathcal{P}_1}\mathbf{E}_{\mathcal{P}_2,\mathcal{F}_1})^T \quad (12)$$

It is in [8] that the oblique projection is first applied in SIMO system for simultaneous channel and symbol estimation. The major difference between the proposed algorithm with the one in [8] is that we only use the row spaces to derive the goal projector while in [8], the Toeplitz structure of the input matrix is further exploited to remove the remaining ISI after oblique projection.

The Algorithm: The Geometry Recall from (9) that the current observation satisfies

$$\mathbf{X}_{L+1}(t+L) = \underbrace{\mathbf{hs}_t + \mathbf{p}_1}_{\mathbf{p}_2} + \mathbf{f}_1 = \mathbf{p}_2 + \mathbf{f}_1, \quad (13)$$

$$= \underbrace{\mathbf{hs}_t + \mathbf{f}_1}_{\mathbf{f}_2} + \mathbf{p}_1 = \mathbf{f}_2 + \mathbf{p}_1. \quad (14)$$

These quantities are illustrated in Figure 3, where subspaces are represented as directed lines or planes, such as $\mathcal{P}_2, \mathcal{P}_1, \mathcal{R}\{\mathbf{hs}_t\}$, while matrices or data are represented as vectors with specific lengths, such as $\mathbf{p}_2, \mathbf{p}_1, \mathbf{X}_{L+1}(t+L)$. To obtain $\mathbf{hs}_t = \mathbf{p}_2 - \mathbf{p}_1$, we obtain $\mathbf{p}_i$ from decompositions in (13-14) using two oblique projections sequentially. From the plane $\overline{ACFH}$ in Figure 3, because $\mathbf{p}_2 \in \mathcal{P}_2$ and $\mathbf{f}_1 \in \mathcal{F}_1$, $\mathbf{p}_2$ can be obtained by the oblique projection of $\mathbf{X}_{L+1}(t+L)$ onto $\mathcal{P}_2$ along $\mathcal{F}_1$, *i.e.*,

$$\mathbf{p}_2 = \mathbf{X}_{L+1}(t+L)\mathbf{E}^T_{\mathcal{P}_2,\mathcal{F}_1}.$$

Now from the plane $\overline{ABCD}$, $\mathbf{hs}_t$ can be obtained from the oblique projection of $\mathbf{p}_2$ onto $\mathcal{F}_2$ ($\overline{ABGH}$) along $\mathcal{P}_1$, *i.e.*,

$$\mathbf{hs}_t = \mathbf{p}_2\mathbf{E}^T_{\mathcal{F}_2,\mathcal{P}_1} = \mathbf{X}_{L+1}(t+L)(\mathbf{E}_{\mathcal{F}_2,\mathcal{P}_1}\mathbf{E}_{\mathcal{P}_2,\mathcal{F}_1})^T.$$

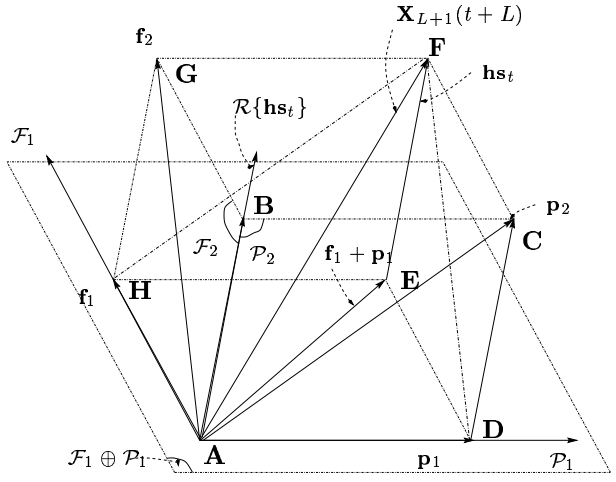

Figure 3: Channel and Symbol Estimation by Projection

Order Detection For multipath channels with small head and tail taps, it is desirable to have order detection capability. We now consider the subspaces when the channel order is over or under determined as L'. The corresponding *future* and *past* data are represented in Fig. 4. Notice when $L' \neq L$, the condition in Lemma 1 is not satisfied, hence the projection result will not be the outer-product of the channel vector $\mathbf{h}$ and the symbol sequence $\mathbf{s}_t$. Define the following matrix:

$$\mathbf{G_I} \triangleq \mathbf{E}_{\mathcal{F}_2,\mathcal{P}_1}\mathbf{E}_{\mathcal{P}_2,\mathcal{F}_1} + \mathbf{E}_{\mathcal{P}_2,\mathcal{F}_1}\mathbf{E}_{\mathcal{F}_2,\mathcal{P}_1},$$

where the subspaces are defined using L'. The following proposition establishes an order detection algorithm:

Proposition 1 *Let* $\mathbf{E}'_t \triangleq \mathbf{X}_{L'+1}(t+L')\mathbf{G}_I^T$ *then under noiseless condition,* $rank(\mathbf{E}'_t) = 1$ *if and only if* $L' = L$*; otherwise* $rank(\mathbf{E}'_t) > 1$.

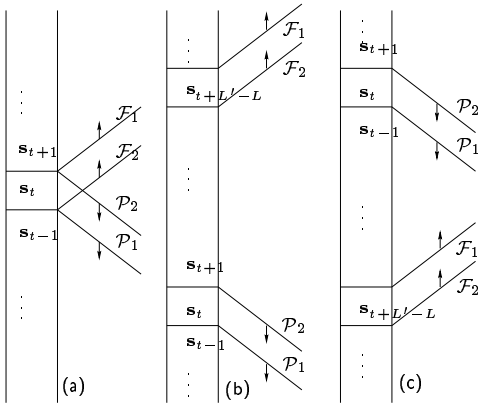

Figure 4: (a) Correct order; (b) Over-determined order;(c) Under-determined order

Thus, in practice, an order detection method by checking the rank of $\mathbf{E}'_t$ numerically can be implemented before channel coefficients estimation. We omit the formal proof (See [9]) but provide some insights by considering three separate scenarios.

Remarks:

- Case I: $L = L'$ shown in Fig. 4(a). In this case, $\mathbf{G}_I$ is still a projector because $\mathbf{E}_{\mathcal{F}_2,\mathcal{P}_1}$ and $\mathbf{E}_{\mathcal{P}_2,\mathcal{F}_1}$ commute. So the projection $\mathbf{E}'_t$ will have rank one.
- Case II: $L > L'$ shown in Fig. 4(b). Here $\mathcal{F}_2$ and $\mathcal{P}_2$ don't have an intersection. When $\mathbf{E}_{\mathcal{F}_2,\mathcal{P}_1}\mathbf{E}_{\mathcal{P}_2,\mathcal{F}_1}$ is applied to $\mathbf{X}_{L'}(t+L')$, the only remaining part in the row space is $\mathbf{s}_t\mathbf{E}^T_{\mathcal{F}_2,\mathcal{P}_1}$. On the other hand, if $\mathbf{E}_{\mathcal{P}_2,\mathcal{F}_1}\mathbf{E}_{\mathcal{F}_2,\mathcal{P}_1}$ is applied, $\mathbf{s}_{t+L'-L}\mathbf{E}^T_{\mathcal{P}_2,\mathcal{F}_1}$ will be left. So in general, $\mathbf{E}'_t$ has exactly rank two.
- Case III: $L < L'$ shown in Fig. 4(c). In this case, $\mathbf{E}_{\mathcal{F}_2,\mathcal{P}_1}\mathbf{E}_{\mathcal{P}_2,\mathcal{F}_1}$ and $\mathbf{E}_{\mathcal{P}_2,\mathcal{F}_1}\mathbf{E}_{\mathcal{F}_2,\mathcal{P}_1}$ are not well-defined because their range and null spaces are not disjoint. Detailed analysis [9] will show the two projectors map the data matrix into two non-zero matrices but with different row space, hence the summation of the projections has rank no less than two.
- In practice, the numerical rank checking is done by comparing the ratios of the second largest singular value to the largest singular value for orders from one to a given upper bound. The order achieving the smallest ratio is the detected order. This has the advantage that the subjective thresh-hold selection is avoided. The disadvantage, however, is its high computation complexity due to using SVD.

IV. Variations

Besides the sequential projection algorithm $\mathbf{E}_I \triangleq \mathbf{E}_{\mathcal{P}_2,\mathcal{F}_1}\mathbf{E}_{\mathcal{F}_2,\mathcal{P}_1}$, the geometrical representation in Fig. 3 directly yields two variations of the algorithm:

1. Assume that we have $\mathbf{p}_2$ and $\mathbf{p}_1$. Then $\mathbf{hs}_t$ is given by $\mathbf{p}_2 - \mathbf{p}_1$. This is illustrated in the triangle $\widehat{\mathbf{ACD}}$: $\mathbf{DC} = \mathbf{AC} - \mathbf{AD}$. The corresponding projector is $\mathbf{E}_{II} \triangleq \mathbf{E}_{\mathcal{P}_2,\mathcal{F}_1} - \mathbf{E}_{\mathcal{P}_1,\mathcal{F}_2}$, *i.e.*,

$$\mathbf{hs}_t = \mathbf{X}_{L+1}(t+L)\mathbf{E}^T_{II}.$$

This procedure can also be done with $\mathbf{f}_2$ and $\mathbf{f}_1$.

2. Assume we have $\mathbf{f}_1, \mathbf{p}_1$. Then $\mathbf{hs}_t$ is given by $\mathbf{X}_{L+1}(t+L)-(\mathbf{f}_1+\mathbf{p}_1)$. The relation is ready to show in the triangle $\widehat{\mathbf{AEF}}$: $\mathbf{EF} = \mathbf{AF} - \mathbf{AE}$. The corresponding projector is $\mathbf{E}_{III} \stackrel{\Delta}{=} \mathbf{I} - (\mathbf{E}_{\mathcal{P}_1,\mathcal{F}_2} + \mathbf{E}_{\mathcal{F}_1,\mathcal{P}_2})$, i.e.

$$\mathbf{hs}_t = \mathbf{X}_{L+1}(t+L)\mathbf{E}_{III}^T.$$

Some useful remarks are given below:

Remarks:

- Note that by claiming the combination (summation and difference) of two projectors are still projector, we need to prove some conditions on the the projectors should be satisfied as in Lemma 1. We refer readers to [4] for details.
- Under the noiseless condition, the projector $\mathbf{E}_{III}$ is the same as $\mathbf{E}_{II}$, since $\mathbf{E}_{\mathcal{P}_2,\mathcal{F}_1} = \mathbf{I} - \mathbf{E}_{\mathcal{F}_1,\mathcal{P}_2}$. But in practice, they have different performances due to the presence of the additive noise.
- In deriving all these three projectors, the underlying idea is to remove in $\mathcal{C}$ the vectors contained in $\mathcal{P}_2$ and $\mathcal{F}_2$. This is consistent with LSS [10], where $\mathcal{P}_2$ and $\mathcal{F}_2$ are removed by the use of orthogonal projection. But by orthogonal projection the remaining part in $\mathcal{C}$ is the projection error $\tilde{\mathbf{s}}_t$, which makes LSS lose the finite sample convergence property in symbol estimation.

V. Simulation Example

In this section, we present two simulation examples on channel and symbol estimation by the proposed algorithms and some existing deterministic algorithms: "SS-Channel" [3], "SS-Symbol" [7], "LSS" [10], "J-LSS" [6] and "OB-PM" [8]. Algorithms are compared by Monte Carlo simulations. We use normalized root mean square error (NRMSE) for channel estimation and root mean square error (RMSE) per symbol for symbol estimation. The input sequence is an i.i.d. equally probable quadrature phase shift keying (QPSK) complex sequence.

Randomly Generated Channel In our first example, we demonstrate the performances of the proposed algorithms for well-conditioned channels with known channel order. The channels are randomly generated by the following three steps: (1). Generate $L+1$ tap coefficients according to i.i.d. Gaussian distribution; (2). Interpolate the channel according to the output number P (over-sampling rate); (3). Normalize the channel to $||\mathbf{h}|| = 1$. In this example, $L = 5$ and $P = 2$. 500 channels are used for each SNR and 100 symbols are used for each Monte Carlo runs.

The performance curves for channel and symbol estimation are shown in Fig. 5, 6. It appears that all these deterministic channel estimation algorithms perform almost the same, and indeed the differences among the curves disappear after 60 dB.

It is interesting to point out that "SS-symbol" [7] outperforms the other algorithms by 5 dB in high SNR region. Our explanation is, in oblique projection based algorithms, symbols are estimated by forming the intersection of two subspaces $\mathcal{F}_2$ and $\mathcal{P}_2$, while in "SS-symbol", symbols are obtained by intersecting of all subspaces containing $\mathbf{s}_t$.

Multipath Channel In the second example, we present the simulation results for multipath channels. The channel used here is the same as the one from [6]. The over-sampling rate is 2 and the tap number is 5. 200 Monte Carlo runs are used for each SNR and 100 symbols are used for each run. The performance curves are plotted in Fig. 7 and 8.

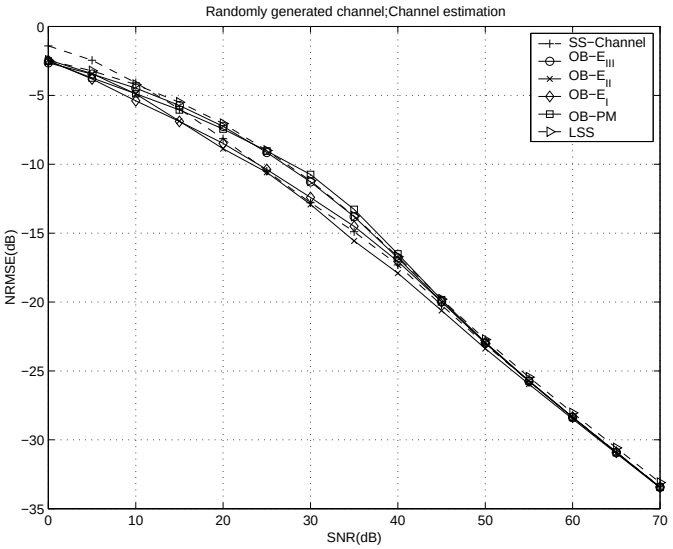

Figure 5: Randomly generated channel: channel estimation

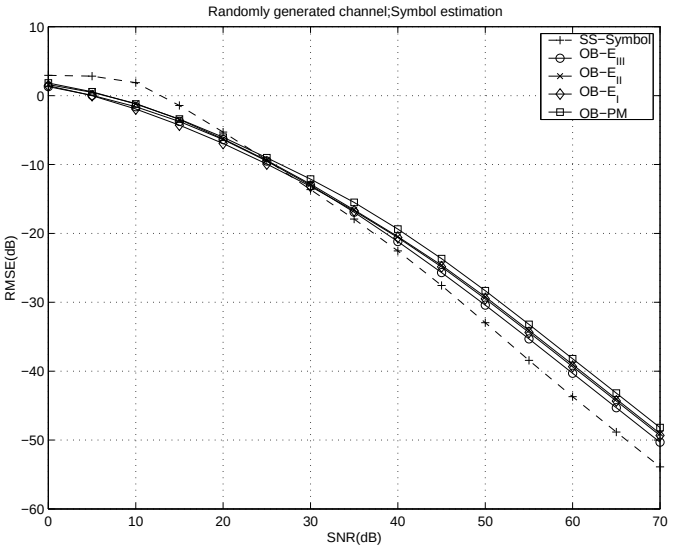

Figure 6: Randomly generated channel: Symbol estimation

From Fig. 7, 8, It can be seen that the proposed order detection scheme together with the corresponding projector considerably outperforms those without order detection capability. And it also performs better than J-LSS[6] for SNR less than 30 dB. In high SNR region, the curve finally coincides with other deterministic methods when the order is correctly chosen.

VI. Conclusions

Blind channel and symbol estimation algorithms for a SIMO system are considered in this paper. Based on (1) the isomorphic relationship between the input and output spaces; (2) oblique projection of the observation onto signal and interference subspaces, we derived three new projectors to estimate the channel and the symbols simultaneously. These deterministic algorithms possess the critical property of finite sample convergence both in channel and symbol estimation, which is highly desirable for

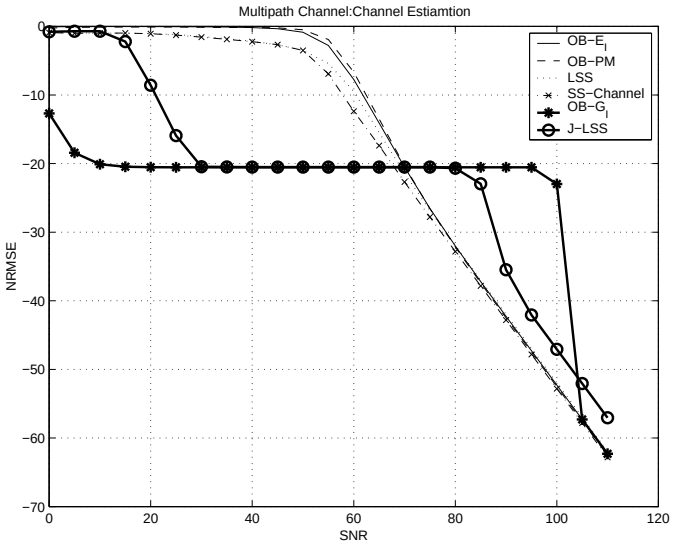

Figure 7: Multipath channel: Channel estimation

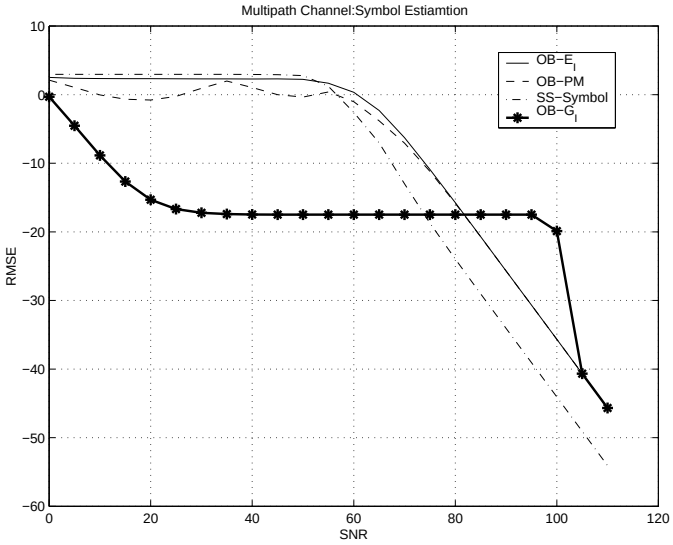

Figure 8: Multipath channel: Symbol Estimation

short data sample applications. Together with the estimation algorithms, a new order detection scheme is developed. The simulation results show the efficiency of the proposed algorithms, especially for multipath channels. The main shortcoming of the algorithms is the computation burden due to the use of singular value decomposition.

References

[1] R. T. Behrens and L. L. Sharf. "Signal processing applications of oblique projection operators". *IEEE Trans. Signal Processing*, 42(6):1413 – 1424, June 1994.

[2] R.E. Blahut. *Algebraic Methods for Signal Processing and Communications Coding*. Springer-Verlag, New York, NY, 1992.

[3] E. Moulines, P. Duhamel, J.F. Cardoso, and S. Mayrargue. "Subspace-Methods for the Blind Identification of Multichannel FIR Filters". *IEEE Trans. SP*, SP-43(2):516–525, Feb. 1995.

[4] C. R. Rao and S. K. Mitra. *Generalized Inverse of Matrices and its Applications*. John Wiley & Sons, Inc., New York, NY, 1971.

[5] L. Tong and S. Perreau. "Multichannel blind channel estimation: From subspace to maximum likelihood methods". *IEEE Proceedings*, 86(10):1951–1968, October 1998.

[6] L. Tong and Q. Zhao. "Joint Order Detection and Blind Channel Estimation by Least Squares Smoothing". *IEEE Trans. Signal Processing*, 47(9), Sept. 1999.

[7] A. van der Veen, S. Talwar, and A. Paulraj. "A subspace approach to blind space-time signal processing for wireless communication systems". *IEEE Trans. Signal Processing*, SP-45(1):173–190, Jan 1997.

[8] P. Vandaele and M. Moonen. "Two deterministic blind channel estimation algorithms based on oblique projections". *Technecal Report(ftp.esat.kuleuven.ac.be/pub/sista/)*, 1999.

[9] X. Yu and L. Tong. "Blind Channel and Symbol Estimation Based on Oblique Projection". *in preparation*, 2000.

[10] Q. Zhao and L. Tong. "Adaptive Blind Channel Estimation by Least Squares Smoothing". *IEEE Trans. Signal Processing*, 47(11), Nov. 1999.